

Constraining the Outburst Properties of the SMBH in Fornax A through X-ray, Infrared, and Radio Observations

L. Lanz, C. Jones, W.R. Forman, M.L.N. Ashby, R. Kraft, R.C. Hickox

Harvard-Smithsonian Center for Astrophysics

llanz@cfa.harvard.edu



Abstract

Combined Chandra, Spitzer, XMM-Newton, and VLA observations of the nearby ($D_L = 22.7$ Mpc (Tonry et al. 2001)) giant radio galaxy NGC 1316 (Fornax A) show features indicative of an AGN outburst most likely **triggered at least 0.4 Gyr ago** by a merger with a galaxy with a stellar mass of $0.9\text{--}7.8 \times 10^{10} M_\odot$. X-ray cavities in the Chandra and XMM-Newton images likely result from the radio jet and the expansion of the radio lobes. The dust emission seen at 5.8, 8.0, and 24 microns is strongest in the regions with little or no radio emission, suggesting that the expanding radio plasma removes or destroys the dust as well as the hot gas. These results constrain properties of the outburst and the merger galaxy. The size of the X-ray cavities implies a **minimum outburst energy of 1.2×10^{58} ergs**. The present size of the radio lobes, spanning $33'$ (215 kpc) (Ekers et al. 1983) implies that the outburst is at least 0.4 Gyr old. The inferred dust mass implies that the **merger galaxy was a late-type spiral with a stellar mass of $0.9\text{--}7.8 \times 10^{10} M_\odot$ and a gas mass of $0.4\text{--}4.4 \times 10^{10} M_\odot$** .

Infrared Morphology

NGC 1316 was observed as part of the Spitzer SINGS Legacy program (Kennicutt et al. 2003). At $3.6 \mu\text{m}$ and $4.5 \mu\text{m}$, its emission is dominated by stellar light. We fit all the images using GALFIT (Peng et al. 2002) with a Sérsic profile and a central point source, using the $3.6 \mu\text{m}$ image to fit the shape of the Sérsic profile used to model the stellar emission. Input and residual images are shown in Figure 1. The remaining structure is primarily due to dust emission. Aside from emission in the nuclear region, the dust appears to be **concentrated in two irregular regions**, one $23.8''$ (3.1 kpc in the plane of the sky) southeast of the nucleus and the other extending $43.9''$ (4.8 kpc) to the northwest and forming a clumpy arc.

5.8 micron 8.0 micron 24 micron

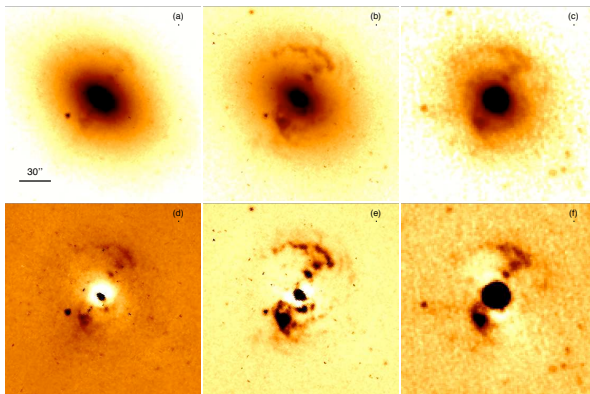


Fig. 1 Spitzer images at 5.8 μm (a), 8.0 μm (b), and 24 μm . (c) (log scale) and their residual images (linear scale) once the Sérsic profile modelling the stellar light has been removed. The residual emission shows the clumpy distribution of the dust.

X-ray and Radio Morphology

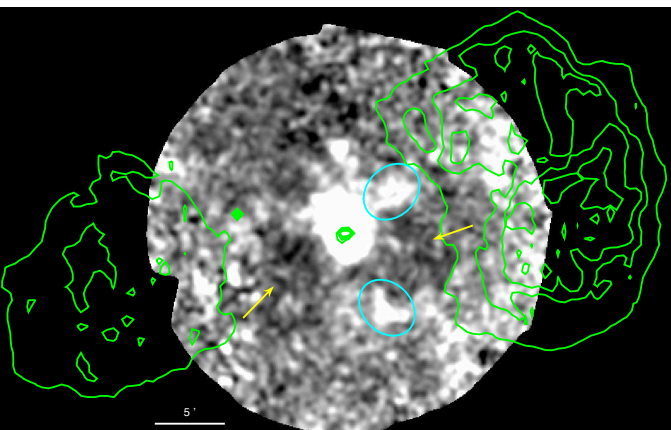


Fig. 2 (above)

The XMM soft (0.5–2.0 keV) exposure-corrected image shows cavities in the X-ray emission to the west and southeast (yellow arrows). Their existence is confirmed by the azimuthal profile (Fig. 3) which shows the lowest emission at 0° and 210° . The western cavity is more clearly delineated by the bright rims circled in blue. The green contours show radio lobe emission at 20 cm (Fomalont et al. 1989).

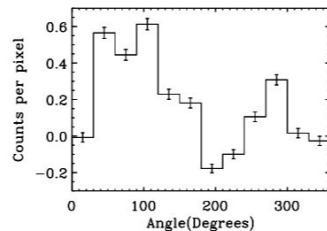


Fig. 3 (below) Azimuthal profile of a $125''\text{--}375''$ annulus of the XMM image (West is 0° and North is 90°) showing the same cavities as Figure 2 at 0° and 210° .

Multi-wavelength Comparison of Features

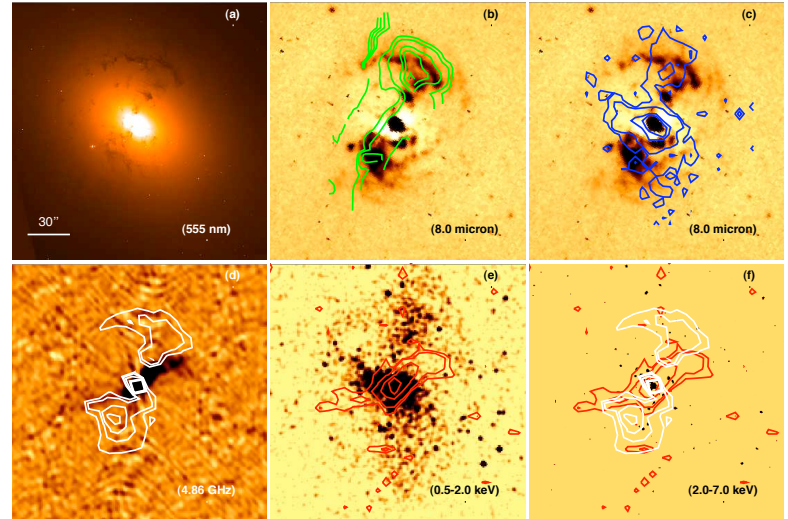


Fig. 4 (a) Hubble (555 nm), (b,c) non-stellar 8 micron, (d) VLA (4.86 GHz), (e) soft (0.5–2.0 keV) Chandra, and (f) hard (2.0–7.0 keV) Chandra images overlaid with 8 micron (white), CO(2–1) (green), soft X-ray (blue), and radio (red) contours.

Figure 4 shows the emission at various wavelengths. Infrared dust emission (b, c, white) coincides with molecular emission (green) (Horellou et al. 2001) and optical dust extinction (a), but not with the radio jet emission (d, f, red). Panel e demonstrates that the radio jet coincides with the cavity seen in the soft X-ray emission. This small inner cavity is not resolved in the XMM image (Fig. 2). The soft X-ray emission (blue contours in c) is strongest in regions lacking dust emission to the east, south-west, and north of the nucleus. These images suggest that the **radio jet creates the inner X-ray cavity** and that dust and molecular gas survive longest where X-ray emission is weakest and the radio jet cannot remove or destroy it.

Results: Outburst Properties

The Spitzer observations show dust emission concentrated in two regions (Fig. 1) that coincide with CO(2–1) emission (Fig. 4b). The soft X-ray observations show cavities (Fig. 2, 4e) produced by the radio plasma. From the Fornax A multi-wavelength observations, we constrain the mass of the merger galaxy as well as the outburst age and kinetic energy:

- **Progenitor Mass:** following Patil et al. (2007), we predict the equilibrium dust mass within 5 kpc of the nucleus to be $1.3 \times 10^4 M_\odot$. Our photometry of the Fig.1 features agrees with that predicted by Draine et al. (2007) who calculate a much larger total dust mass of $3.2 \times 10^7 M_\odot$. From the excess dust, we estimate the merging galaxy had to be a spiral galaxy with a stellar mass of $0.9\text{--}7.8 \times 10^{10} M_\odot$, assuming a dust-to-stellar mass ratio between $0.4\text{--}3.4 \times 10^{-3}$. Using the M/L ratio of Bell et al. (2003) and the gas-mass-to- L_B relations of Bettoni et al. (2003) and assuming typical galaxy colors (Trimble, 2000), we estimate a merger galaxy cold gas mass of $0.5\text{--}4.4 \times 10^{10} M_\odot$. Since NGC 1316 has a cold gas mass less than $1.3 \times 10^9 M_\odot$ (Kennicutt et al. 2003, Horellou et al. 2001), some cold gas must be lost in the merger event.
- **Outburst Age:** assuming that the merger fueled the outburst, a lobe expansion speed of $0.6 c_s$, and a gas temperature of 0.77 keV (Isobe et al. 2006), the projected lobe extent of ~ 100 kpc on the sky implies an outburst age of at least 0.4 Gyr.
- **Outburst Energy:** from the volume of the western X-ray cavity and assuming isothermal gas, and adiabatic bubble expansion, we can set a lower limit of 1.2×10^{58} ergs on the outburst energy.

References

- Bell, E. F. et al. 2003, ApJS, 149, 289
 Bettoni, D. et al. 2003, AA, 405, 5
 Draine, B. et al. 2007, ApJ, 663, 866
 Ekers, D. et al. 1983, AA, 127, 361
 Fomalont, E. et al. 1989, ApJ, 364L, 17
 Forman, W. et al. 2007, ApJ, 665, 1057
 Horellou, C. et al. 2001, AA, 376, 837
 Isobe, N. et al. 2006, ApJ, 645, 256
 Kennicutt, R. et al. 2003, PASP, 115, 928
 Patil, M. et al. 2007, AA, 461, 103
 Peng, C. et al. 2002, AJ, 124, 266
 Tonry, J. et al. 2001, ApJ, 46, 681
 Trimble, V. 2000, in Allen's Astrophysical Quantities, ed. A.N. Cox (New York: Springer-Verlag), 569